Near DC Eddy Current Measurement of Aluminum Multilayers using MR Sensors and Commodity Low Cost Computer Technology

Alexander R. Perry

PAMURRAY, San Diego, CA 92192-7104, USA

ABSTRACT

Low Frequency Eddy Current (EC) probes are capable of measurement from 5 MHz down to DC through the use of Magnetoresistive (MR) sensors. Choosing components with appropriate electrical specifications allows them to be matched to the power and impedance characteristics of standard computer connectors. This permits direct attachment of the probe to inexpensive computers, thereby eliminating external power supplies, amplifiers and modulators that have heretofore precluded very low system purchase prices. Such price reduction is key to increased market penetration in General Aviation maintenance and consequent reduction in recurring costs.

This paper examines our computer software CANDETECT, which implements this approach and permits effective probe operation. Results are presented to show the intrinsic sensitivity of the software and demonstrate its practical performance when seeking cracks in the underside of a thick aluminum multilayer structure. The majority of the General Aviation light aircraft fleet uses rivets and screws to attach sheet aluminum skin to the airframe, resulting in similar multilayer lap joints.

Keywords: NDE Eddy Current Low Frequency Magnetoresistive sensors Aluminum Multilayers

1. INTRODUCTION

Magnetoresistive (MR) sensors have a useful frequency response from $1\,Hz$ through $5\,MHz$ without needing special techniques.[1] Inductive coil sensors can also cover that range of frequencies, but generally not in a single sensor. One probe sensor can cover a range of one or two orders of magnitude, before a differently designed sensor would offer significantly improved performance. The limitation on broadband performance has precluded use of some techniques for inherent elimination of lift-off from results.

Some applications need narrowband low frequency performance to achieve sufficiently deep penetration of ferromagnetic[2] or highly conductive[3] materials. Measurements with magnetoresistive sensors have previously been reported using Honeywell,Kodak[4] and NVE[5] commercial devices, requiring expensive external amplifiers and/or acquisition equipment. Our approach avoids such additional equipment because it would increase the future system price to beyond the range acceptable to the target user audience.

High grade computer sound cards have a frequency response from $50\,Hz$ through $15\,kHz$ with full performance[6] which, while narrow compared to MR performance, is sufficient for many new applications. Below that frequency range, the needed time to make a measurement becomes significant and may preclude practical use in the field. Faster sample rate sound cards (and dedicated data acquisition cards) can reach higher frequencies,[7] as may be needed for low conductivity materials. Some new software that operates a computer sound card was connected to an MR-based eddy current probe and the effective sensitivity examined by inspecting a test sample that already has reported[4] results.

2. THE SOFTWARE - CANDETECT

CANDETECT[8] provides a software framework for sending a waveform to a probe and recording the response waveform. The library *AudNet* operates the soundcard and a modified version of *xoscope* displays the streaming results.

E-mail: alex.perry@ieee.org

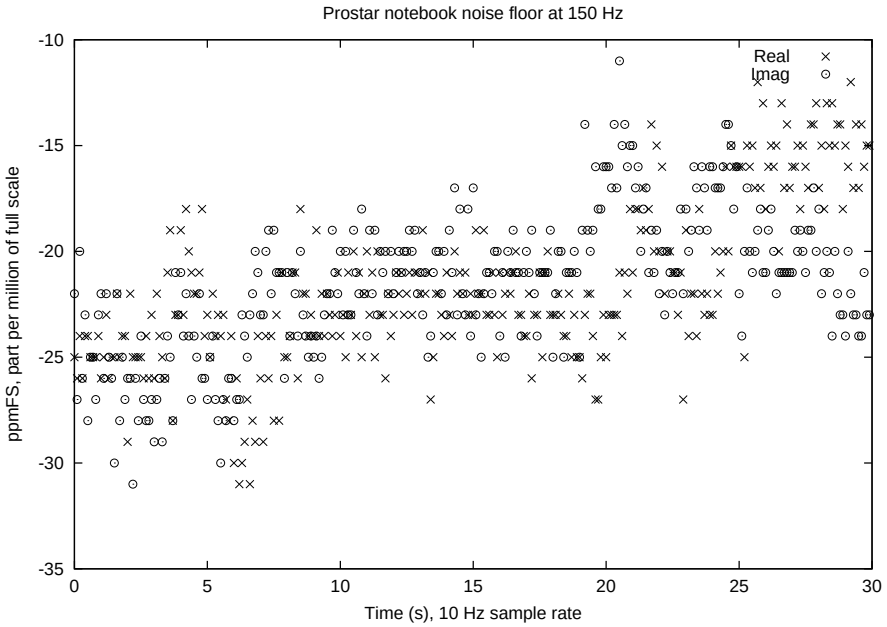

Figure 1: Prostar notebook with disconnected input - Noise floor

2.1. AudNet

The library operates the sound card. It ensures that there is always a sufficient backlog of outgoing audio data that the sound card will never have to pause, since this would impair the quality of the measurement. It also retrieves the recorded signals, as soon as the sound card makes them available, and processes the raw waveforms to a consistent state. Clients submit requests for measurements, which are performed as soon as possible, then collect the responses from a queue. Many different kinds of measurement request can be submitted at any time, the library simply works through the to-do queue until it gets to the end (if it ever does). When the request queue becomes empty, the most recent request is repeated until a new one shows up.

Each request consists of one waveform for every electrical output channel available, normally two for most sound cards, together with the number of times that the waveform should be repeated. When the request is performed, all the incoming signals are collected into a response for the client. The response contains one waveform for each electrical input channel, also normally two for most sound cards, with the requested repetitions averaged together so that the output and input waveforms have the same length and timing characteristics. Since many electromagnetic systems are slightly resonant, the request also specifies how many times the waveform must be performed until the probe and sample have reached a predictable state for reliable measurement. These skipped cycles are only performed when the library switches from one request to a different request definition; they are not needed when a request repeats. All input and output values are scaled so that full scale is $-1 \ldots +1$ in the waveforms.

Since playback data has to be placed into the sound queue a second or more before it is played, and recorded data appears in the sound queue a short time after it is recorded, the library keeps track of how much data is in those sound queues. Often, the request being written into the queue is different from the one which is electrically active. That electrically active request may also be different from the one being read from the sound queue and collected into a response. The library hides this underlying complexity from the user clients, but cannot remove the need for clients to select the desired measurements a short time before they will be performed.

2.2. AudNet main program

This program expects the first command line parameter to be a frequency in Hz and the second command line parameter to be the phase adjustment of the output in degrees. It currently requests the library generate a clean sinewave on one speaker channel and a clean cosinewave on the other channel with a frequency that is as close as possible to the requested one, in order to support the alternate probe as discussed in section 4. The library delivers measurement responses about ten times per second.

Whenever a new result is generated, the program writes a line to the standard output and flushes the file to ensure that the recipient receives the result. The line has three numbers, corresponding to the actual frequency, the measured signal at the desired phase and the signal in quadrature to that phase.

Figure 1 shows 30 seconds of data, with a $150\,Hz$ carrier, taken on the Maestro 2E sound chip in a Prostar[10] notebook computer with a disconnected input to establish the noise floor. The data shows offsets of $21.6, 21.5\,ppm$ with drifts of $0.15, 0.11\,ppm/s$ and noise levels of $0.87, 0.86\,ppm/\sqrt{Hz}$ on the Real and Imaginary channels.

2.3. xoscope

The original `xoscope`[9] application is intended for use as an oscilloscope, whereby a hardware driver monitors a signal source for a specified trigger condition and hands a waveform fragment back to the main application. The user interface allows the trigger and plotting parameters to be specified, rather like an oscilloscope, and periodically asks the driver to try to find a new trigger event.

The trouble with this approach, for CANDETECT's purposes, is that a real oscilloscope will discard input signal whenever it is too busy to draw to the screen and the software version does the same thing. This is fine when the goal is to monitor a high speed transient waveform, but problematic for viewing a slowly changing signal over many seconds. Thus, the sound card operation is separated into the *AudNet* `main` program as above. The floating point values are scaled so that one count of the oscilloscope waveform is $10\,ppm$ of the soundcard fullscale input, ensuring little or no loss of signal for the noise levels identified above. In consequence, signals in excess of 32% of fullscale are clipped on the display due to the limited dynamic range of the application's internal storage buffers. If the data is copied to file, between *AudNet*'s `main` and `xoscope`, the recorded values will be neither truncated nor clipped.

3. COMPUTER SYSTEMS

Selection of the computer requires care, but need not be expensive. The measurements reported here were conducted with a year-old Prostar[10] notebook computer and with a *New Internet Computer* (NIC).[11] The latter has a retail price of $200 and includes everything except the monitor.

In order to simultaneously output and input a waveform, the sound card must be capable of full duplex operation. Many older cards, and also more recent notebook computers, are unable to achieve full duplex without reducing the sample resolution and/or sample rate. The card needs to operate in 16 bit mode, whereby each voltage reading is nominally capable of resolving $16\,ppm$ of full scale. In practice, the electrical noise, both the card itself and the interior of the computer, impose a practical $100\,ppm$ limit per reading. Increasing the rate at which readings are taken will spread that noise across a wider bandwidth, diluting it at whatever the desired frequency is. Even a card that cannot exceed the CDROM sample rate of $44100\,Hz$ is thus capable of $1\,ppm$ with a $4\,Hz$ measurement update rate.

The NIC contains the CM8738 chip manufactured by C-Media,[6] offering $1.1\,V_{rms}$ with $80\,dB$ signal-to-noise ratio that corresponds to the $100\,ppm$ above. The line output can drive $32\,\Omega$ and the microphone input has a $\times 10$ gain. The Prostar contains the ES1978 chip "Maestro 2E" from ESS Technology that has comparable capabilities, for this application.

4. PROBE DESIGN

Honeywell sensors electrically appear to be a resistive bridge, just under $1200\,\Omega$ per leg, achieving $1\,mV/V/G$ at $55\,^oC$ and better at lower temperatures. A four times transformer improves the match to most sound cards, which expect a load around $80\,\Omega$, so that $4\,V_{RMS}$ may be applied to the sensor. The resulting signal from the sensor is best amplified using another four times transformer to increase the sensor's source impedance of $600\,\Omega$ to $10\,k\Omega$ and convert the differential signal into the ground-referenced single ended high impedance voltage expected by the sound card. In conjunction with the $20\,dB$ gain that is usual for most microphone inputs, the system can measure $6\,G, 0.6\,mT$ signals (full scale) without external powered active components.

Conventionally, the sensor bridge has a constant voltage applied across it, such that the output signal is proportional to the magnetic field. The electrical noise associated with low frequency operation impairs performance, so a higher signal to noise ratio can be attained by modulating the magnetic signal into the optimal performance band of the sound card input amplifier. The actual frequency to be used is different for each sound card and needs to be measured during initial system configuration, taking into account the performance of the two transformers. Once the frequency is determined, the appropriate sound card channel is instructed to generate that waveform continuously.

The magnetic excitation field that illuminates the sample is generated by the second sound card output. Since this field must be generated at the desired measurement frequency, transformers cannot be used to match the impedance. Depending on the probe design, the available field strength will differ; a conventional current sheet probe, for example, can readily achieve $0.1\,G_{RMS}$ on most sound cards.

No other electronics are needed to operate the probe, so it is unpowered and can readily be used in conjunction with a notebook computer that is mobile and running on batteries. A probe implementing those characteristics is currently under development, but is delayed due to parts availability lead times and was not completed in time to take data for inclusion in this paper.

For the results described herein, the Kodak-based alternate probe[4] was exclusively used. This includes a powered bridge excitation circuit and a bridge preamplifier, thus making it impossible to modulate the magnetic signal to a higher frequency. The associated loss of performance counteracts the benefits of an external bridge preamplifier to boost signal strength.

5. RESULTS

The test sample consists of three stacked aluminum plates. Each plate contains two rows of fastener holes, which run parallel to the plate edges. The first row is $0.540", 13.7\,mm$ from the nearest edge of the top plate, and the second row is $0.710", 18\,mm$ from the first row. The seven fastener holes in each row are separated by $1.250", 31.7\,mm$, and the fasteners in the second row are offset from the holes in the first row by $0.140", 3.6\,mm$ in the direction parallel to the rows. The middle plate, $0.500", 12.7\,mm$ thick, is sandwiched between upper and lower plates 0.250" (6.3 mm) thick. The middle plate is offset from the other two, so that one of its long edges extends $1.000", 25.4\,mm$ beyond the edges of the top and bottom plates, to represent one side of the lap joint. The holes in the top plate are countersunk to accommodate steel taper-lock fasteners.

To simulate buried cracks, the underside plate contains a slot, radiating from the central fastener hole in a direction parallel to the nearby edge of the plate. The slot was produced by electrical discharge machining (EDM) and is approximately $0.010", 0.25\,mm$ wide, $0.375", 9.5\,mm$ long and passes through the full $0.250", 6.3\,mm$ thickness of the plate. Figure 2 shows the signal from that cracked plate at $150\,Hz$ when the two obscuring plates are removed, with no phase correction or balancing.

For the second scan, all three plates were stacked together with the fasteners in place. Measurements were made simultaneously at four frequencies $20\,Hz$, $30\,Hz$, $40\,Hz$ and $90\,Hz$ using the multiple waveform capabilities of the library. The raw data is shown in Figure 3, demonstrating that the fasteners continue to dominate the waveforms. The steel fastener can be readily rejected by correlation, since its signal is in-phase, independent of frequency and will dominate relative to the eddy current signal for the lowest frequency. Deep cracks are apparent at low frequencies, with a phase lag on the signal that is frequency dependent. They are hidden from higher frequencies by the penetration depth so that the difference between penetrating and non-penetrating

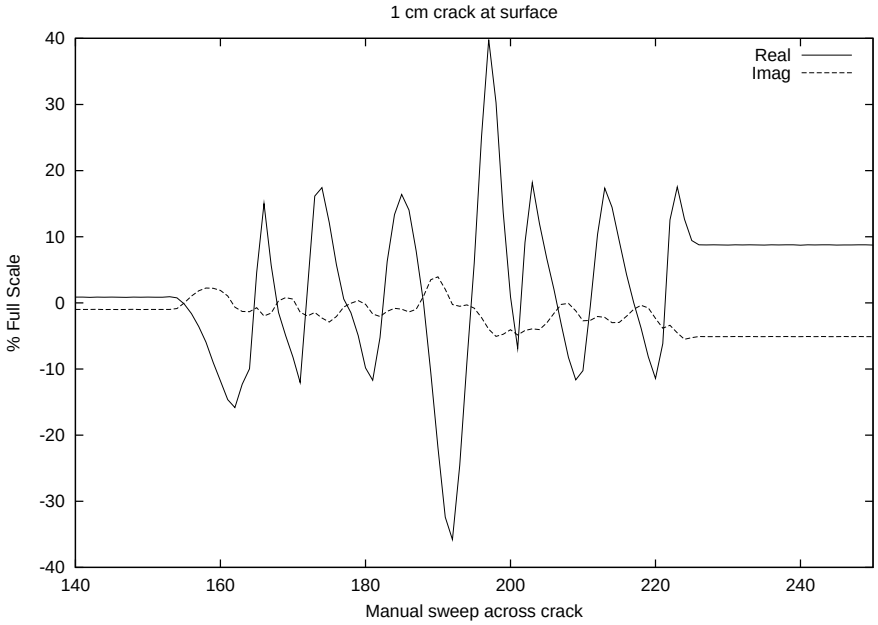

Figure 2: Prostar notebook, sample plate, surface crack

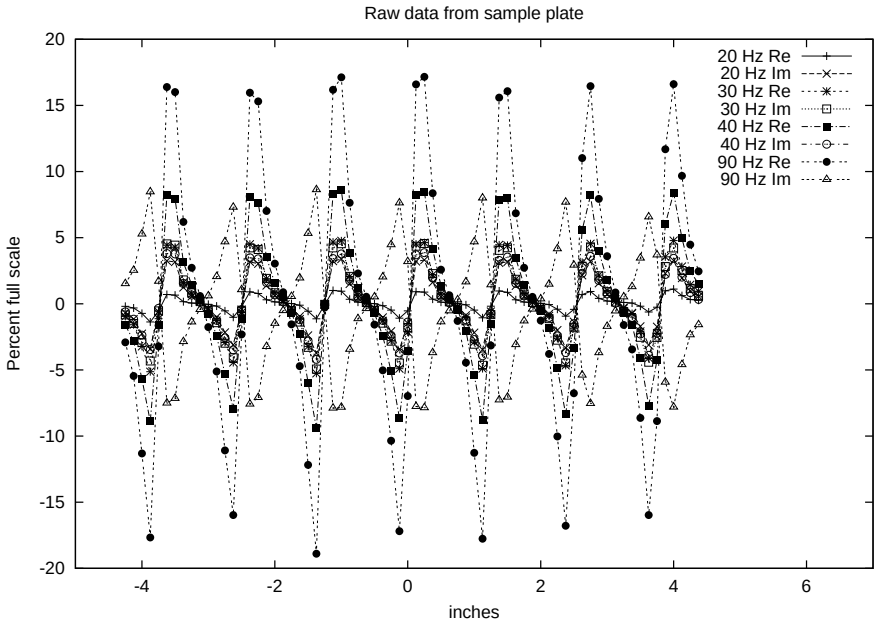

Figure 3: Prostar notebook, sample plate, buried crack, raw data

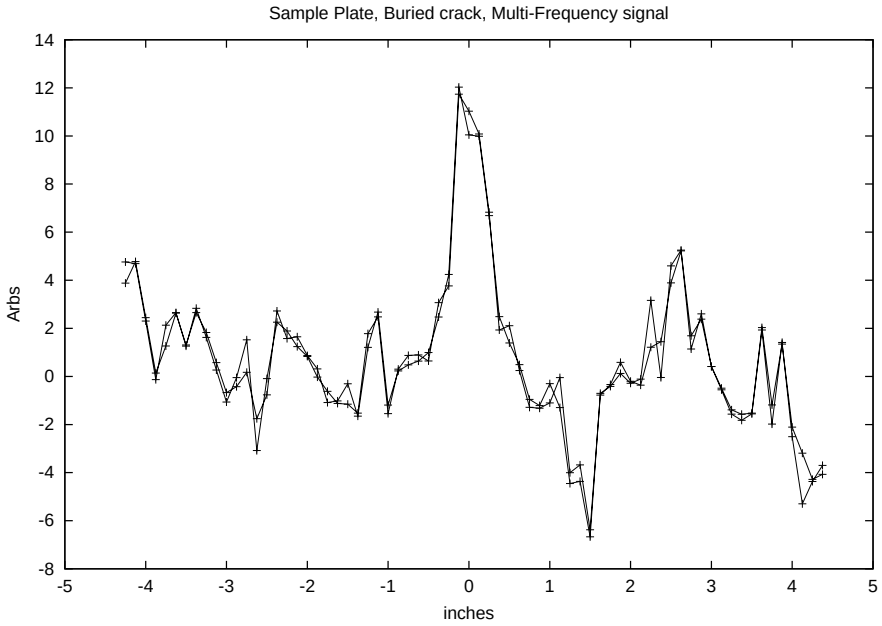

Figure 4: Prostar notebook, sample plate, buried crack, processed

frequencies can be used to measure (and reject) undesired variations of surface properties. This method is implemented by the relative gains and phases in Table 1, taking into account the gain and phase characteristics of the sound card at low frequency.

Table 1: Gain and phase coefficients for multi-frequency detection.

$20\,Hz$	3.3	21.7^o
$30\,Hz$	-52.6	52.4^o
$40\,Hz$	25.0	-9.6^o
$90\,Hz$	-26.5	-8.7^o

Figure 4 shows the resulting signal variation with scan position for two sets of measurements. The positive peak around zero clearly indicates that there is an anomalous decrease in reactive response of $11\,arbs$ for frequencies around $30\,Hz$. The anomaly is consistent between the two data sets and is localized around the actual position of the buried crack.

The similarity of the two sets of measurements, indicating the underlying sensor noise, has a standard deviation of $0.6\,arbs$. The position-dependent variation of the measurements, indicating sample-induced effects, has a standard deviation of $2.3\,arbs$. Both of these are much smaller than the signal peak and the signal to noise ratio $SNR \approx 5$ suggests that deep cracks as small as $0.075", 2\,mm$ may be detectable with unity signal to noise ratio in a single inspection scan.

Both surface and buried cracks scans were detected with signals of spatial width about $0.750", 2\,cm$.

The probe was used to manually scan the lower side of the right wing of a Cessna 172 aircraft, outboard of the strut mounting point for approximately $60\,cm$ of track. Figure 5 shows the region being inspected, with the probe passing right-to-left along the row of rivets above the lip of the lap joint. The track starts to the right of the right hand access panel at $25\,arbs$, passes the right row of rivets at $34\,arbs$ and the left row at $46\,arbs$. The

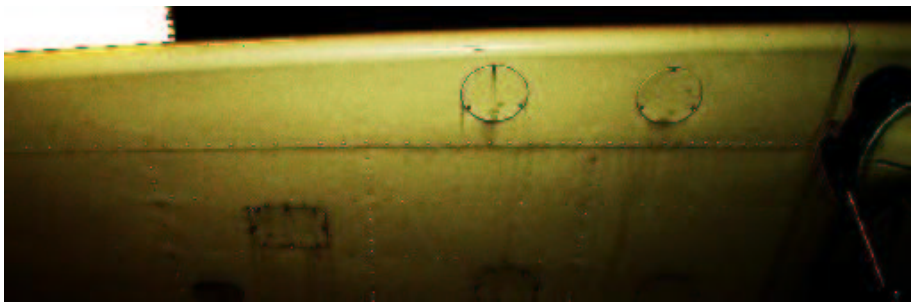

Figure 5: Cessna 172 right wing from below

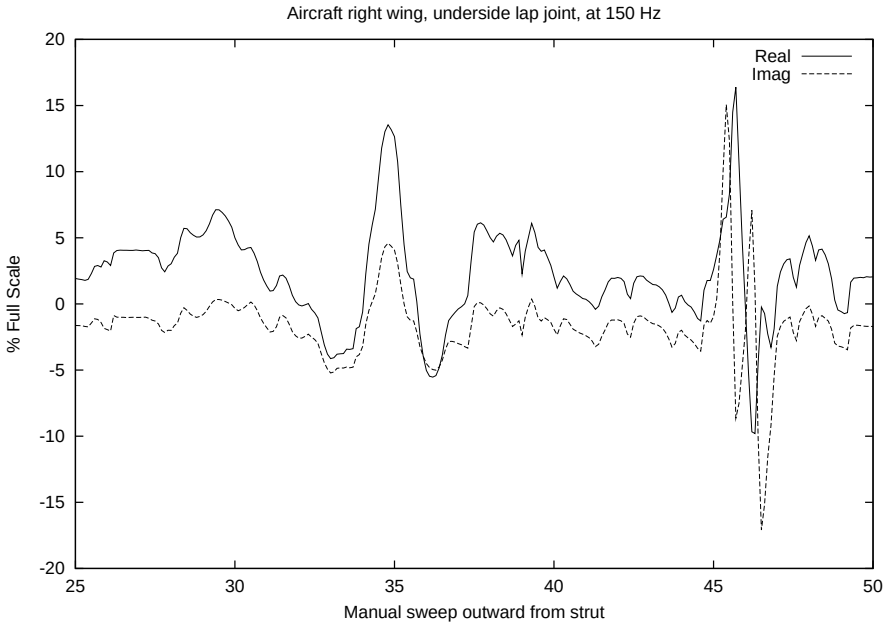

Figure 6: Prostar notebook, right wing spar from below

horizontal axis in the plots is actually 25 s of time. The manual movement achieved approximately 1 $s/rivet$ so that the time axis approximately counts rivets along the track.

Figure 6 shows the raw results, taken using the higher 150 Hz frequency that is appropriate for the thinner metal sheets in light aircraft. Spatial filtering and phase selection was used to separate that data into two slowly varying components in Figure 7 and two high resolution components in Figure 8. The filter cutoff is set for two rivet spacings, to ensure that any crack signals will appear in the high resolution components.

The first and second components, at phase angles of 60^o and 40^o, show that the structure behind the two rivet lines consists of different materials, due to the different phase angles of the resulting signal. The third component, at a phase angle of 0^o, shows the residue from the rivets that was imperfectly rejected by the probe's design. This component can be used, by counting peaks, to determine exactly where a given time instant of the signal originated on the inspection track. The fourth component, at a phase angle of -45^o, would report any cracks between the fasteners, either under the paint or in the underlying structures. There is no transient, comparable in size to the test sample signals, along the majority of the track.

The fourth component in Figure 8 does have one visible transient at the 46 $arbs$ rivet line, somewhat smaller than would be expected from a crack like the test sample. The details of the hidden structure have not been

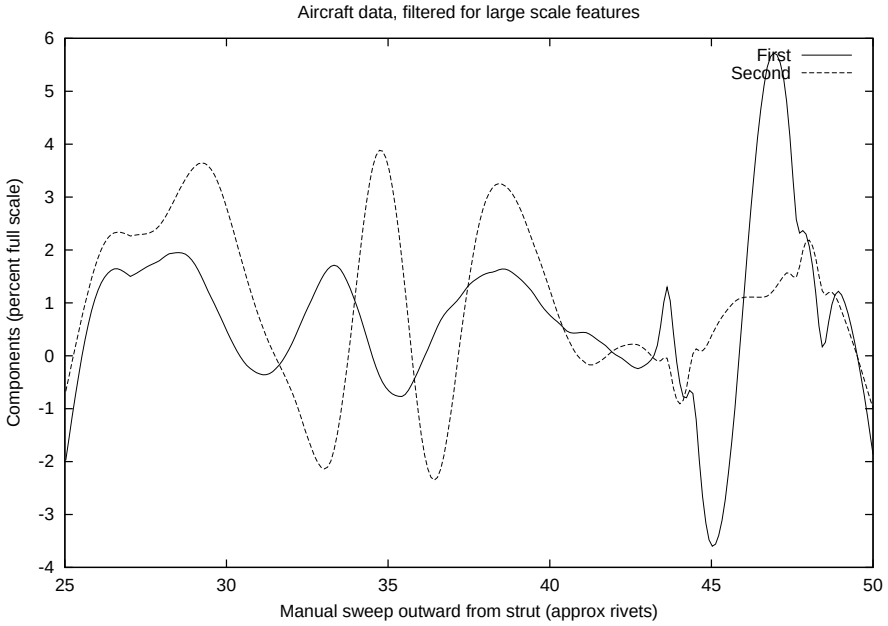

Figure 7: Aircraft and prostar notebook, low spatial frequency signal components

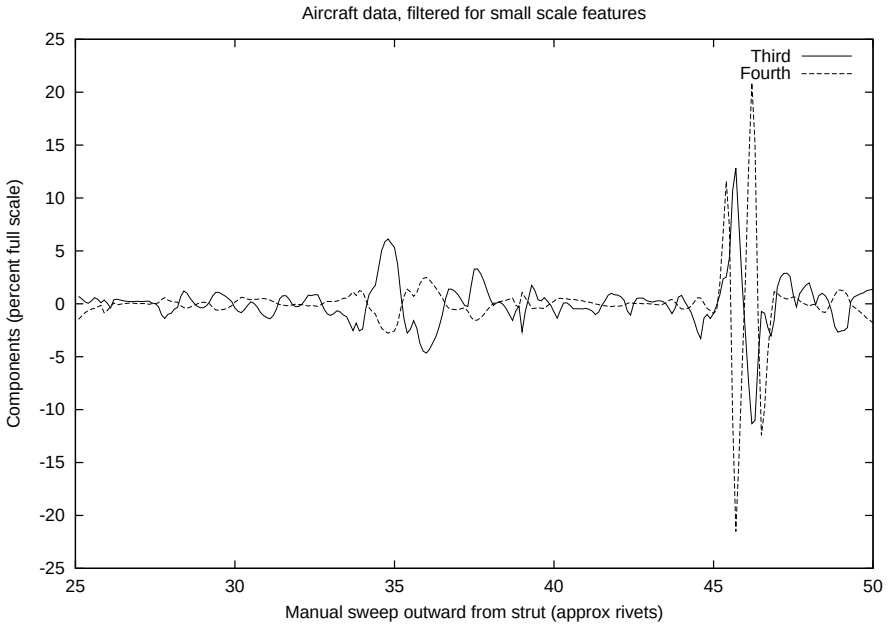

Figure 8: Aircraft and prostar notebook, high spatial frequency signal components

verified at this time, but the signal is consistent with the end of a sheet of material.

6. CONCLUSIONS

When operated within the frequency and signal strength ranges that were anticipated by the manufacturer, conventional computer sound cards are shown to achieve sub-ppm performance levels. This is demonstrated to be sufficient for low frequency NDE needs.

Magnetoresistive sensor based eddy current probes can be operated without loss of performance by a computer with the CANDETECT software, greatly reducing the cost of such systems.

ACKNOWLEDGMENTS

The probe and sample used for these measurements was graciously loaned by *Dr. W.F. Avrin.* Laboratory space for system integration was provided by *Quantum Magnetics* (San Diego) and workshop space for evaluation with aircraft was provided by *El Cajon Flying Service.* Their assistance in this work is greatly appreciated.

REFERENCES

1. HMC1023 chip, `http://www.ssec.honeywell.com/magnetic/features_comp.html#hmc1023`, Honeywell Solid State Electronics Center, 12001 State Highway 55, Plymouth, MN 55441-4799
2. A.R. Perry, P.V. Czipott, A.L. Singsaas, W.F.Avrin, P. Meilland and F. Midroit, "Low frequency electromagnetic sensing of cracks and inclusions in ferromagnetic materials using magneto-resistive sensors," Proc. SPIE 3586 *Nondestructive Evaluation of Aging Aircraft, Airports and Aerospace Hardware III*, 154-164, 1999.
3. Y. Dalichaouch, A. L. Singsaas, F. Putris, A. R. Perry, and P. V. Czipott, "Low frequency electromagnetic technique for nondestructive evaluation," Proceedings of SPIE, *Nondestructive Evaluation of Aging Aircraft, Airports, and Aerospace Hardware IV* (March 2000, Newport Beach, CA), 2-9, 2000.
4. W.F. Avrin, "Eddy-current measurements with magnetoresistive sensors" in proceedings *Nondestructive Evaluation of Aging Aircraft, Airports and Aerospace Hardware IV* edited by *A.K Mal* in vol. 3994 pp. 29-36, 2000.
5. T. Dogaru and S.T. Smith, "Giant Magnetoresistance-Based Eddy Current Sensor", *IEEE Trans Magnetics* Volume 37, No 5 pp. 3831-8, 2001.
6. `http://www.cmedia.com.tw/doc/cmi8738.doc` C-MEDIA ELECTRONICS INC., 6F, 100, Sec 4, Civil Boulevard, Taipei, Taiwan, R.O.C..
7. `http://www.measurementcomputing.com/cbicatalog/cbiproduct.asp?dept%5Fid=139&pf%5Fid=1098`
8. `http://candetect.sourceforge.net/`
9. Under ongoing development at `http://xoscope.sourceforge.net/`
10. Prostar Computer Inc, 1128 Coiner Ct., City of Industry, CA 91748
11. `http://www.thinknic.com` "The New Internet Computer Company" 781 Beach Street, 4th Floor, San Francisco, CA 94109